

EXPLICITLY DESCRIBING FIBERED 3-MANIFOLDS THROUGH FAMILIES OF SINGULARLY FIBERED SURFACES

MAGGIE MILLER

ABSTRACT. We give an explicit description of a fibration of the complement of the closure of a homogeneous braid, understanding how each fiber intersects every cross-section of S^3 .

1. INTRODUCTION

In this note, we give an explicit description of a fibration of the complement of the closure of a homogeneous braid (e.g. a torus knot). These links have long been known to be fibered, since Stallings [Sta78] observed that a standard Seifert surface for such a link decomposes into a Murasugi sum of fiber surfaces for torus knots.

Abstractly proving the existence of a fibration on a knot or link complement is generally straightforward, since (for example) fiberedness is detected by knot or link Floer homology [Ni07]. However, the author of this paper usually finds it difficult to conceptualize the whole fibration of such a link complement in total, rather than a single fiber. While building fibrations in a 4-dimensional setting, we found that a deeper understanding of fibrations of classical knot complements seemed necessary in order to extrapolate to higher dimensions. We thus worked to explicitly describe how the fibers of certain link complements meet every cross-section of a standard Morse function on S^3 .

We first give an imprecise statement of the main theorem, meant to illustrate the aim of the paper.

Theorem 1.1. *Let L be the closure of a homogenous braid β . Then L is a fibered link and we can explicitly describe a fibration $F : S^3 \setminus \nu(L) \rightarrow S^1$. The level sets of F are simple, in the sense that there is a natural Morse function h on (S^3, L) so that for every $\theta \in S^1$, the restriction of h to the interior of $F^{-1}(\theta)$ has no local minima or maxima.*

The proof of Theorem 1.1 is an explicit construction, which we are sharing with the belief that this can motivate arguments in 4-dimensional (or higher) manifolds where the usual techniques in 3-dimensional topology fail. (In the

2020 *Mathematics Subject Classification.* 57K30.

The author is supported by a Clay Research Fellowship and a Stanford Science Fellowship.

author's mind, this paper is mostly an exposition on the structure of a fibration of a 3-manifold over S^1 .) We focus on closures of homogeneous braids as a natural, well-understood family of fibered links. We obtain a very restrictive statement about the position of the fibers of such a link that might be of interest to knot theorists and 3-dimensional topologists.

We give the precise statement of Theorem 1.1 now, which we will prove constructively in the following sections of this paper.

Theorem 1.2. *Let L be the closure of a homogenous braid β on b strands, braided with respect to the standard Morse function $h : S^3 \rightarrow \mathbb{R}$, with the minima and maxima of h also minima and maxima of $h|_L$. Then there is a fibration $F : S^3 \setminus \nu(L) \rightarrow S^1$ so that simultaneously for all θ , the restriction of h to the interior of $F^{-1}(\theta)$ is Morse with no local minima nor maxima and the restriction of h to the boundary of $F^{-1}(\theta)$ is Morse with b local minima and b local maxima.*

2. BRAID CONVENTIONS

We choose some conventions when discussing links in braid position.

Definition 2.1. Decompose $S^3 = B_+^3 \cup (S^2 \times I) \cup B_-^3$. Let $h : S^3 \rightarrow \mathbb{R}$ be Morse so that h has one local maximum in B_+^3 , one local minimum in B_-^3 and the restriction $h|_{S^2 \times I}$ is projection to I .

Further decompose $S^2 \times I = (D_L^2 \times I) \cup (D_R^2 \times I)$. Let β be a braid in $D_L^2 \times I$ on b strands. Let L be a link with

$$L \cap (D_L^2 \times I) = \beta \quad \text{and} \quad L \cap (D_R^2 \times I) = \{b \text{ points}\} \times I,$$

and so that $L \cap B_+^3$ and $L \cap B_-^3$ each consist of b strands, on each of which h has one local critical point, with two of these extrema being the two critical points of h . We say L is in *braid position with respect to h* and is the *braid closure of β* . See Figure 1.

Recall that a braid diagram of a braid β on b strands can be written as a word in $\sigma_1, \sigma_1^{-1}, \dots, \sigma_{b-1}, \sigma_{b-1}^{-1}$, where σ_i is a diagram involving one positive half-twist between the i -th and $(i+1)$ -th strands and no other crossings, and σ_i^{-1} is similar but with a negative half-twist. We will use the convention that the letters in a word w from left to right describe crossings in a diagram of β from bottom to top. This means that if w_1, w_2 are words for β_1, β_2 , then $w_1 w_2$ is the word for the braid obtained by stacking β_2 above β_1 .

Definition 2.2. A braid is *homogeneous* if it can be written as a word in $\sigma_1^{s_1}, \dots, \sigma_{b-1}^{s_{b-1}}$ for some $s_1, \dots, s_{b-1} \in \{-1, 1\}$, with each letter appearing at least once.

In simpler terms, a braid is homogeneous if it can be written as a braid word so that for each i , the word includes one of σ_i and σ_i^{-1} , but not both. See Figure 1.

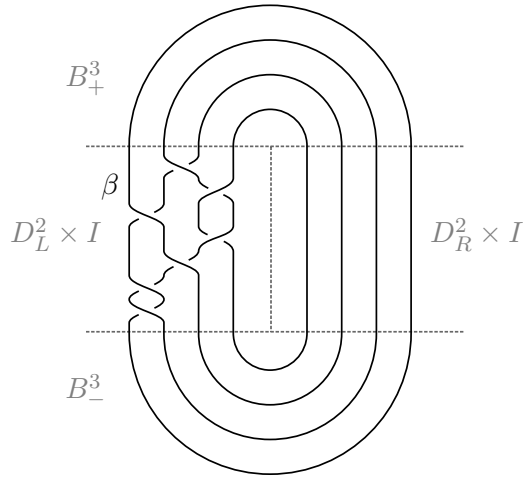


FIGURE 1. A link L in braid position as the braid closure of β . Here, β is a homogeneous braid since its given diagram is described by the braid word $\sigma_1^{-1}\sigma_1^{-1}\sigma_2^{-1}\sigma_3\sigma_1^{-1}\sigma_3\sigma_2^{-1}$, which is a word in the letters $\sigma_1^{-1}, \sigma_2^{-1}, \sigma_3$ with each letter appearing at least once.

3. BACKGROUND: CONSTRUCTING FIBRATIONS

In this section, we discuss local constructions of fibrations in dimension three. Our plan is to fix a height function $h : M^3 \rightarrow \mathbb{R}$ whose regular level sets are surfaces and whose singular level sets are surfaces with well-understood singularities. (In the case that M is closed, h is simply a Morse function.) We will then construct a family of functions f_t mapping each level set $h^{-1}(t)$ to the circle, with rules on how f_t changes with t to ensure that the function $F : M \rightarrow S^1$ given by $F(x) = f_{h(x)}(x)$ is a fibration. The advantage of this approach is that while drawing a collection of surfaces in a 3-manifold may seem daunting, drawing a collection of curves (level sets of f_t) in a surface (a level set of h) may seem more approachable.

Convention 3.1. In this paper, we use the terms “singular fibration” and “height function” rather than “circular Morse function” or “Morse function” on manifolds with boundary to make it clear that we do not expect functions to be locally constant on boundary. For us, a *height function* $h : M \rightarrow \mathbb{R}$ is a smooth function that has the following properties.

- $h|_{\partial M}$ is Morse.
- h is Morse on the interior of M .
- The level sets of h meet ∂M transversely away from critical points of $h|_{\partial M}$.

For example, if L is a link in S^3 and $h : S^3 \rightarrow \mathbb{R}$ is Morse with $h|_L$ also Morse, then h restricts to a height function on $M := S^3 \setminus \nu(L)$ for $\nu(L)$ a suitable tubular neighborhood of L .

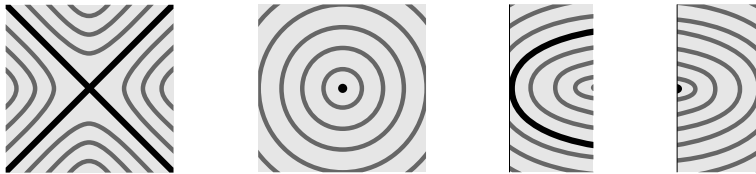


FIGURE 2. Local models near singular points of a leaf of a singular fibration $f : \Sigma \rightarrow S^1$ (away from singularities of Σ). **First:** A leaf includes an \times -singularity. **Second:** A leaf component is a single point in the interior of Σ . **Third:** A leaf has an isolated tangency to $\partial\Sigma$. **Fourth:** A leaf component is a single point in the boundary of Σ .

We first observe that given a fibration $F : M^3 \rightarrow S^1$ and a height function $h : M^3 \rightarrow \mathbb{R}$, we generically expect F to induce a singular fibration on each level set of h .

Definition 3.2. A *singular fibration* on a compact surface Σ is a smooth map $f : \Sigma \rightarrow S^1$ with the following properties.

- The restriction $f|_{\partial\Sigma}$ is Morse.
- For all but finitely many θ , $f^{-1}(\theta)$ is a compact, properly embedded 1-manifold.
- For all θ , $f^{-1}(\theta)$ is a compact, properly embedded 1-manifold away from a finite number of singularities of the four types shown in Figure 2. We will often refer to interior wedgepoints (first image in Figure 2) as *\times -singularities*.

We refer to each $f^{-1}(\theta)$ as a *leaf* of f .

We may extend Definition 3.2 to apply to some singular surfaces. Here, by *singular surface* we mean a compact topological space embeddable in \mathbb{R}^4 containing a finite singularity set S whose complement is a surface.

Definition 3.3. Let Σ be a compact, singular surface with finite singularity set $S = \{p_1, \dots, p_m, q_1, \dots, q_n\}$.

In words, the points p_1, \dots, p_m are the singularities on the boundary of Σ . These points come in three types: some are seemingly interior points that we have artificially declared to be boundary, some are wedge points in $\partial\Sigma$, and others are isolated points that we declare to be in the boundary of Σ . The points q_1, \dots, q_n are the singularities in the interior of Σ . These points come in two types: the singular points of double cones and isolated points that we declare to be in the interior of Σ .

To be precise, we require each p_i to have a neighborhood that is homeomorphic to one of: \mathbb{R}^2 or $\{(x, y) \mid |x| \geq |y|\}$ or $\{(0, 0)\}$, with $p_i \mapsto (0, 0)$. We require each q_i to have a neighborhood that is homeomorphic to one of: $\{(x, y, z) \mid x^2 + y^2 = |z|\}$ or $(0, 0)$, with $q_i \mapsto (0, 0)$.

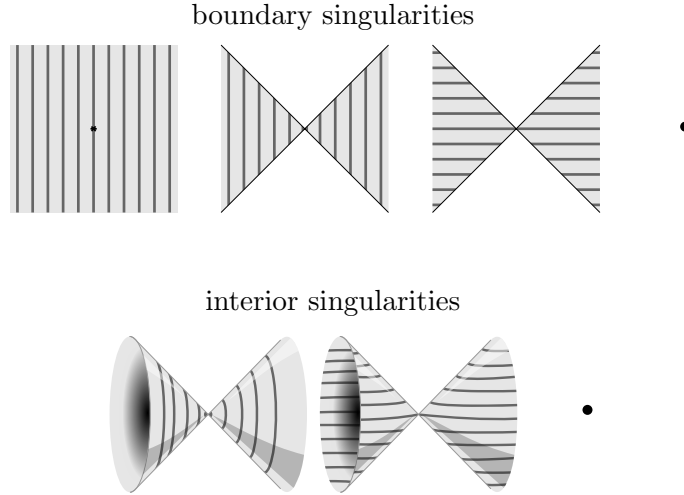


FIGURE 3. Near a singular point of a surface Σ , we require the leaves of a singular fibration f to have one of these pictured local models.

A smooth (away from S) function $f : \Sigma \rightarrow S^1$ is a *singular fibration* if f restricts to a singular fibration on $\Sigma \setminus \nu(S)$ as in Definition 3.2 and in each component of $\nu(S)$, f restricts to one of the local models shown in Figure 3.

In Definition 3.3, we restrict to the given types of singularities precisely because these are the singularities that appear in level sets of a height function $h : M \rightarrow \mathbb{R}$. Interior singular points arise in $h^{-1}(t)$ when the Morse function $h|_{\mathring{M}}$ has a critical point at height t . Boundary singular points arise in $h^{-1}(t)$ when the Morse function $h|_{\partial M}$ has a critical point at height t .

We use singular fibrations of surfaces to construct a fibration of a 3-manifold by considering the level surfaces of a height function.

Definition 3.4. Given a height function $h : M^3 \rightarrow \mathbb{R}$, a *movie of singular fibrations* on M^3 is a family of smooth maps $f_t : h^{-1}(t) \rightarrow S^1$ with each f_t a singular fibration on the singular surface $h^{-1}(t)$ such that the functions f_t vary smoothly with t , i.e. $F(x) = f_{h(x)}(x)$ is a smooth map from M^3 to S^1 . We refer to F as the *total function* of the movie f_t .

By constructing a movie of singular fibrations on M^3 and keeping track of how singular leaves of f_t vary as t increases or decreases, we can arrange for the total function $F : M \rightarrow S^1$ to be a fibration. In [Mil21] we referred to the “type” of singularities in leaves of f_t , determined by the sign of $\frac{d}{dt} f_t$ at that singularity. This language is less useful in this dimension due to symmetry of \times -singularities. (Or in other words, this notation is less useful because an index-1 critical point of a Morse function on a surface remains an index-1 point when turned upside down.) Instead, we add arrow decorations to contour maps of f_t , as shown in Figures 4 and 5. In Figure 5 we draw

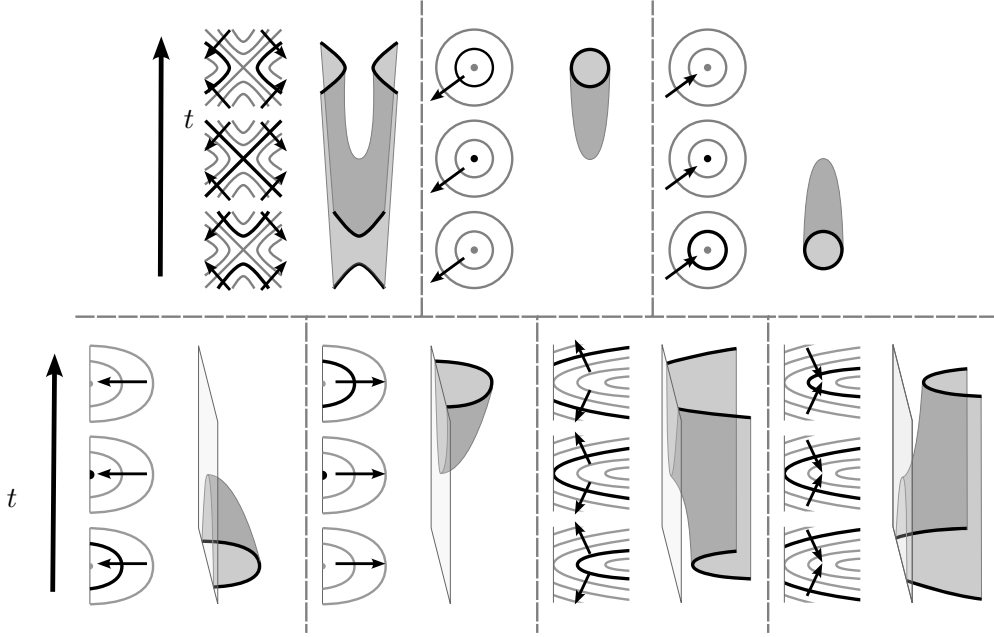


FIGURE 4. Local models near singularities of leaves of f_t that are not also singular points of $h^{-1}(t)$. In all of these models, $\frac{d}{dt}f_t$ is nonzero near the singular point. In each cell, we highlight cross-sections of $F^{-1}(\theta)$ as t increases and give a schematic of $F^{-1}(\theta)$. We include arrows near singularities of leaves of f_t that indicate the behavior of $f_{t\pm\epsilon}$ near the singularity.

only boundary singularities; models of interior singularities can be obtained by doubling.

Proposition 3.5. *The total function F of a movie of singular fibrations f_t is a fibration as long as the following are true.*

- *Near singularities in leaves of f_t that are not also singularities of the surface $h^{-1}(t)$, $\frac{d}{dt}f_t$ is nonvanishing. (That is, we may always draw arrows on contour sets of f_t as in Figures 4 and 5.*
- *At singularities of $h^{-1}(t)$, $\frac{d}{dt}f_t$ vanishes and the arrows decorating $f_{t\pm\epsilon}$ are as in one of the models of Figure 5.*
- *The maps f_0 and f_1 are both fibrations.*

Proof. Assume the listed conditions hold. This ensures that the leaves of F are nonsingular, so $F : M \rightarrow S^1$ is a fibration. \square

Remark 3.6. When the total function F of f_t is a fibration, then h restricts to a height function on each fiber of F . Figures 4 and 5 are simply models of interior and boundary critical points of $h|_{F^{-1}(\theta)}$.

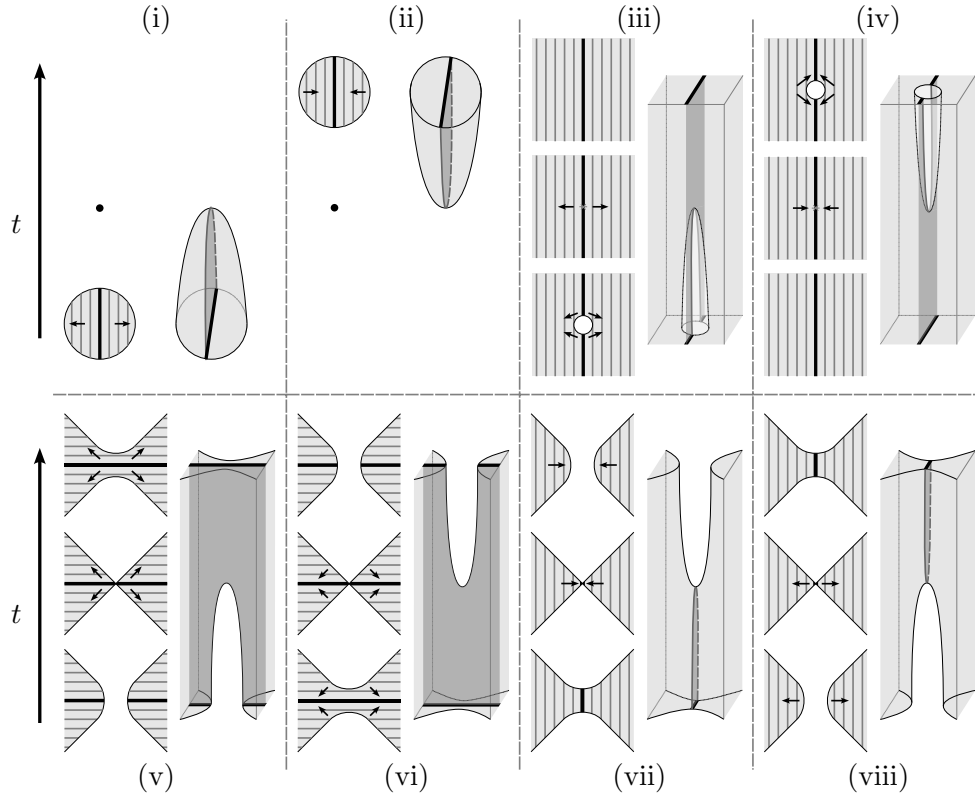


FIGURE 5. Local models near singular leaves of f_t that are also singular points of $h^{-1}(t)$. In each cell, we highlight cross-sections of $F^{-1}(\theta)$ as t increases and give a schematic of $F^{-1}(\theta)$. In each of these models, $\frac{d}{dt}f_t$ is zero at the singular point of $h^{-1}(t)$. We also include arrows in nonsingular cross-sections as in Figure 4. These arrows are drawn assuming that the non-highlighted leaves of F are also locally nonsingular. We draw each singularity as a boundary singularity; doubling these figures yields corresponding local models of singular leaves of f_t with interior singular points.

Notation 3.7. Assume f_t has arrow decorations. A leaf of f_t containing an \times -singularity divides a small neighborhood of that singularity into four regions. Two of these regions (opposite to each other) locally have arrows pointing into them; we call these the *inward regions*. The other two regions locally have arrows pointing away from them; we call these the *outward regions*. See Figure 6.

4. SMALL MOVIES

Here we give three main examples of movies of singular fibrations that we will use to construct more interesting movies. To prove Theorem 1.2, we

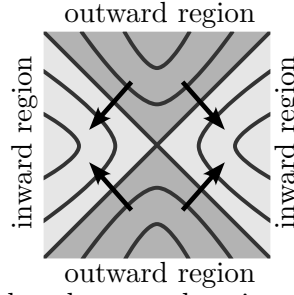


FIGURE 6. Inward and outward regions of a neighborhood of an \times -singularity.

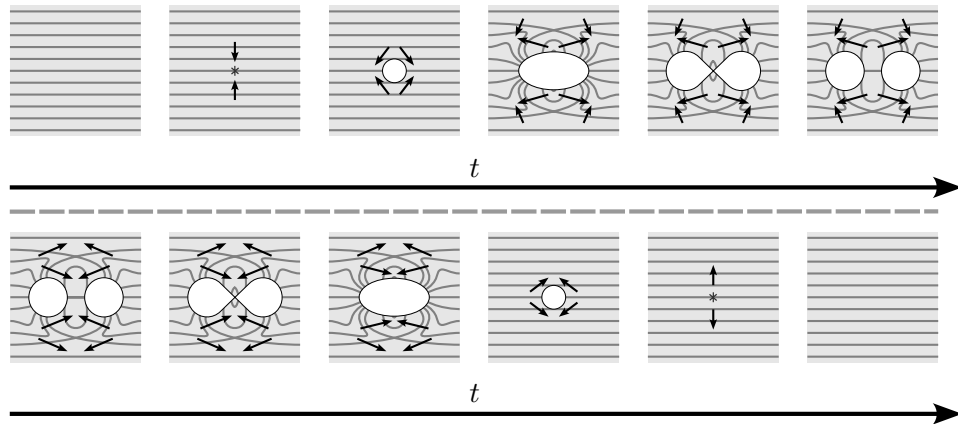


FIGURE 7. **Top row:** the movie of Example 4.1. **Bottom row:** the movie of Example 4.2.

will only need to consider singular fibrations on surfaces with only boundary singularities. From now on, we will only consider singular surfaces with no interior singularities.

Example 4.1. Parametrize a 3-ball B^3 as $I \times I \times I$, and let $\pi : B^3 \rightarrow I$ be projection to the third factor. Fix smooth $f_0 : \pi^{-1}(0) \rightarrow S^1$ so that the level sets of f_0 are lines of the form $0 \times \{I\} \times \{0\}$.

Let γ be an arc properly embedded in B^3 so that $\pi(\partial\gamma) = 1$, and $\pi|_\gamma$ is Morse with exactly one local minimum that is contained in $\pi^{-1}(1/2)$, and projecting γ to $I \times I \times 0$ yields an arc contained in a level set of f_0 .

Let $M^3 = B^3 \setminus \nu(\gamma)$. We choose the thickening of γ so that $h := \pi|_M$ has two singular level sets. See Figure 8. In the top row of Figure 7 we illustrate an extension of f_0 to a movie of singular fibrations $f_t : h^{-1}(t) \rightarrow S^1$. This is a concatenation of movies (iv) and (viii) of Figure 5, so the arrows are consistent with the requirements of Proposition 3.5. The leaves of the resulting total function $F : M \rightarrow S^1$ are nonsingular in their interior, but there are two \times -singularities in leaves of f_1 .

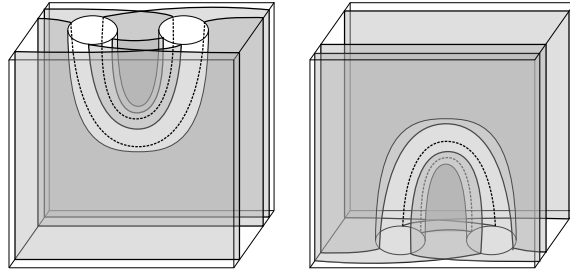


FIGURE 8. Some leaves of the total function of the movies described in Example 4.1 (left) and Example 4.2 (right).

When attempting to fiber the complement of a knot or link L , we can use the movie in Example 4.1 as a model of a fibration near a minimum of L .

Example 4.2. Now we will essentially turn Example 4.1 upside down. Again parametrize a 3-ball B^3 as $I \times I \times I$, and let $\pi : B^3 \rightarrow I$ be projection to the third factor. Let $f_0 : h^{-1}(0) \rightarrow S^1$ agree with the function f_1 of Example 4.1. Fix an arc γ properly embedded in B^3 so that $\pi(\partial\gamma) = 0$, and $\pi|_\gamma$ is Morse with exactly one local maximum that is contained in $\pi^{-1}(1/2)$, and projecting γ to $I \times I \times 0$ yields an arc contained in a level set of f_0 . In the bottom row of Figure 7 we illustrate an extension of f_0 to a movie of singular fibrations $f_t : h^{-1}(t) \rightarrow S^1$. This is a concatenation of movies (vii) and (iii) of Figure 5, so the arrows are consistent with the requirements of Proposition 3.5. The leaves of the resulting total function $F : M \rightarrow S^1$ are nonsingular in their interior, but there are two \times -singularities in leaves of f_0 .

When building a fibration of a knot or link in braid position, we will use the movie in the following example as a model of the fibration near a crossing. It may be helpful to think of a braid closure as obtained by performing band surgeries on an unlink, with bands corresponding to crossings in the braid. In the following example, we show how to change $f_t^{-1}(\theta)$ by band surgery to the leaves along an arc η (the core of a band) as t increases from 0 to 1, assuming that f_0 is sufficiently nice. Since we will use this model several times, we will refer to the movie of Example 4.3 as a *band movie*. We suggest that the reader consider Figure 9 before reading the text of Example 4.3: we draw an arc η connecting one leaf of f_0 to itself, such that the arc crosses over exactly one \times -singularity, meeting the outward regions. We then build a movie of singular fibrations in which the arc is contracted, so that in f_1 , each leaf of f_0 that met η has been changed by some number of band surgeries.

Example 4.3. Parametrize a 3-ball M^3 as $I \times I \times I$, and let $h : M^3 \rightarrow I$ be projection to the third factor. Let $f_0 : \pi^{-1}(0) \rightarrow S^1$ be smooth so that f has one \times -singularity at a point p . Fix arrow decorations at p . Let η be an arc in $I \times I = h^{-1}(0)$ with $\eta(1/2) = p$, meeting the outward regions near

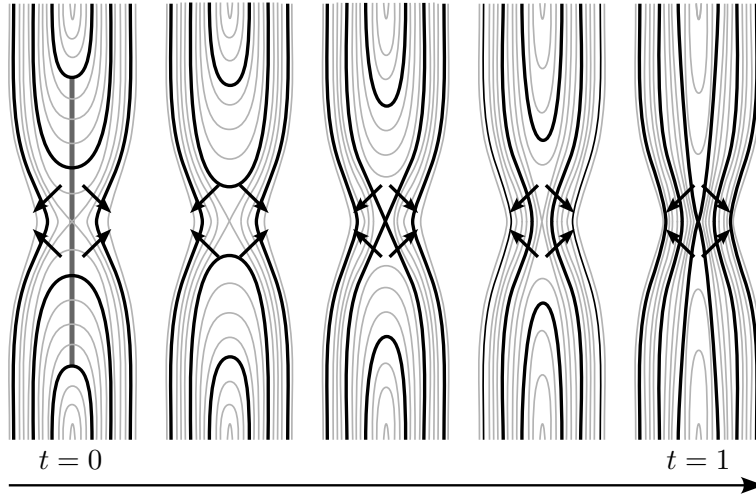


FIGURE 9. The movie of Example 4.3 (band movie). **Left-most frame:** A neighborhood of the arc η (bold vertical arc) in the domain of f_0 . The \times -singularity p of f_0 lies at the center of η . Also in bold, we draw the leaf $f_0^{-1}(\theta)$ that contains the endpoints of η . The leaf $f_0^{-1}(\theta)$ may intersect η in more points as shown (or even include the point p). The circular length condition on η ensures that η intersects $f_0^{-1}(\theta)$ the same number of times on either side of p . **From left to right:** f_t for increasing t .

p . (Recall arrows near \times -singularities point out of outward regions and into inward regions.) Take η to be transverse to all leaves of f_0 away from p . Assume $f_0(\eta(0)) = f_0(\eta(1)) = \theta$ for some θ and that in the intervals $[0, 1/2]$ and $[1/2, 1]$, $f_0 \circ \eta$ winds in equal magnitude about S^1 . That is, assume there is an $l \in \mathbb{R}$ with

$$l = \int_0^{1/2} f_0(\eta(t)) dt = - \int_{1/2}^1 f_0(\eta(t)) dt.$$

Let $b : I \times I \rightarrow I$ be a bump function supported on a small neighborhood of η , with $b(\eta) = 1$. Then set

$$f_t(x) = f_0(x) - t \cdot l \cdot b(x).$$

We draw f_t in Figure 9. Note that $f_1(p) = f_0(p) - l = \theta$. Our requirement that η pass through the outward regions near p ensures that the decoration arrows on f_0 actually correspond to the movie f_t .

Since this movie satisfies the first two conditions of Proposition 3.5, the total function F has leaves that are nonsingular away from $h^{-1}(\{0, 1\})$.

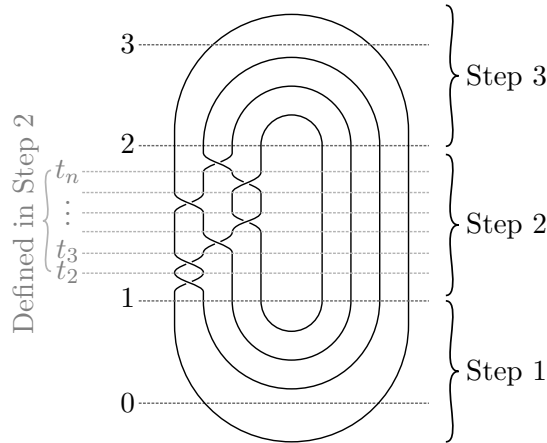


FIGURE 10. A schematic of the values of $h|_M$ relevant to each step of the construction in Theorem 1.2.

5. PROOF OF THEOREM 1.2

Finally, we will re-prove the result of Stallings [Sta78] by explicitly constructing a fibration on the complement of any homogenous braid closure. From now on, let L be a link in braid position as the closure of a homogeneous braid β on b strands. Let $w = w_1 \cdots w_n$ be a homogenous braid word for β , so $w_1, \dots, w_n \in \{\sigma_1^{s_1}, \dots, \sigma_{b-1}^{s_{b-1}}\}$ for some $s_1, \dots, s_{b-1} \in \{-1, 1\}$, with each $\sigma_i^{s_i}$ appearing at least once in w .

Since L is in braid position we have a decomposition $S^3 = B_+^3 \cup (S^2 \times I) \cup B_-^3$, where L meets $S^2 \times I$ in β and a trivial b -stranded braid, while L meets each of B_+^3 and B_-^3 in a trivial b -stranded tangle. The unique minimum of the standard Morse function $h : S^3 \rightarrow \mathbb{R}$ is in B_-^3 and is also a minimum of L , while the unique maximum is in B_+^3 and is a maximum of L .

Isotope as necessary so that the minima of L are in ascending order according to the projection of β described by w . That is, from bottom to top, the i -th minimum of L lies below the i -th endpoint of $\beta \cap \partial B_-^3$. Similarly isotope the maxima to be in descending order, so from top to bottom the i -th maximum of L is in the strand above the i -th endpoint of $\beta \cap \partial B_+^3$. (This is illustrated in Figure 10.)

Reparametrize h so that $h^{-1}((-\infty, 0])$ and $h^{-1}([3, \infty))$ are both balls meeting L in a single arc, and so that $h^{-1}(1) = \partial B_+^3$ while $h^{-1}(2) = \partial B_-^3$. (Again, see Figure 10.)

We will build a movie of singular fibrations on $M^3 := S^3 \setminus \nu(L)$ with respect to $h|_M$ whose total function has nonsingular leaves as in Proposition 3.5 and satisfies the conditions of Theorem 1.2, thus proving Theorem 1.2. In Figure 10, we give a schematic of the position of L and which portions of M are fibered in each step of the construction.

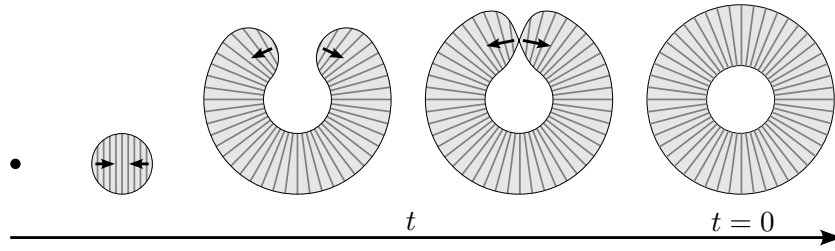


FIGURE 11. The movie f_t for $t \leq 0$. The domain of f_1 is the annulus $h|_M^{-1}(1) \setminus \nu(L)$, i.e. a 2-sphere with neighborhoods of two points in L deleted. Every leaf of f_0 is an arc between these two points (restricted to M). This movie is a concatenation of movies (ii) and (viii) of Figure 5.

5.1. **Step 1: fibering $B_-^3 \setminus \nu(L)$.** Since $h|_M^{-1}((-\infty, 0])$ is a solid torus, it can be fibered by meridional disks. Define f_t for $t \leq 0$ so that the total function from $-\infty < t \leq 0$ is this meridional disk fibration, as in Figure 11. We call the two boundary components of $h|_M^{-1}(0)$ by the names C_1 and C'_1 .

Now we extend f_t across all of $B_-^3 \setminus \nu(L)$. The reader may find it helpful to begin by consulting Figure 12, in which we show how to adapt a singular fibration of a planar surface (in this case, some $h^{-1}(t)$ slightly below a local minimum of $h|_L$) to a planar surface with two additional boundary components (in this case, $h^{-1}(t')$ slightly above a local minimum of $h|_L$).

Note $L \cap B_-^3$ has b components, which we call A_1, \dots, A_b in ascending order. The arc A_1 is the only arc that meets $h^{-1}(0)$. From $t = 0$ to $t = \epsilon$, we extend f_t via isotopy, rotating an arc beneath A_2 by 180° as depicted in Figure 12. The sign of this rotation depends on s_1 . If $s_1 = 1$ (i.e. σ_1 appears in w), then we take the rotation to be counterclockwise, as in the top row of Figure 12. If $s_1 = -1$ (i.e. σ_1^{-1} appears in w), then we take the rotation to be clockwise, as in the bottom row of Figure 12.

We now extend f_t above the minimum of A_2 via the movie of Example 4.1. This adds two new boundary components to the domain of f_t (for the greatest value of t for which f_t is currently defined), which we call C_2 and C'_2 .

Now we can explain why we first performed a 180° rotation. Roughly, we want all boundary components of $h^{-1}(t)$ in the “left” half of the page to correspond to meridians of strands in the braid β , and the boundary components in the “right” half of the page to correspond to vertical strands, as suggested by Figure 10. The 180° rotation causes the “left” boundaries in Figure 12 to have one sign and the “right” boundaries in Figure 12 to have the opposite. The purpose of having the direction of rotation determined by s_1 will be made clear in the next step.

Repeat for A_i , $i = 3, \dots, b$ (using a rotation of sign s_{i-1}) so that f_t is defined for all $t \leq 1$ and $h|_M^{-1}(1)$ has boundary components $C_1, C'_1, \dots, C_b, C'_b$.

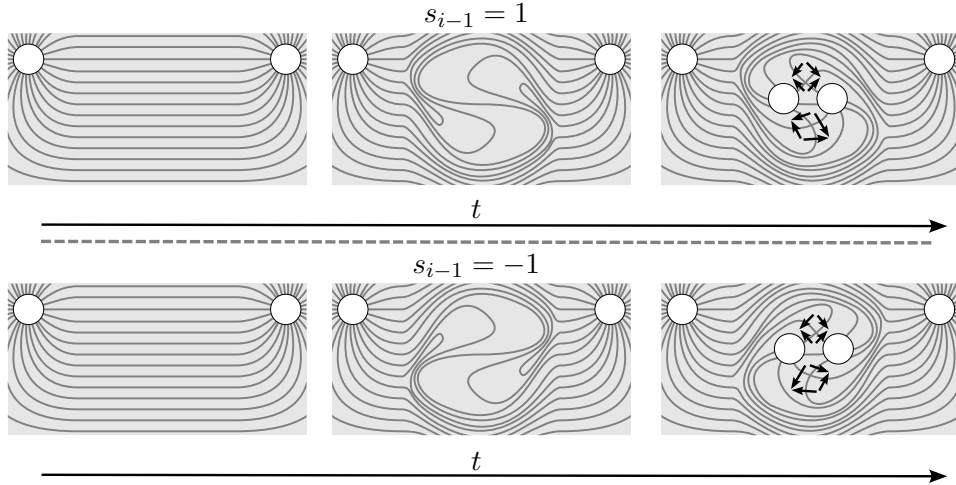


FIGURE 12. An illustration of Step 1. In both rows, we obtain f_t by isotoping f_0 and extending above the minimum of A_i via as band movie (as in Example 4.3). **Top row:** $s_{i-1} = 1$, so we rotate counterclockwise. **Bottom row:** $s_{i-1} = -1$, so we rotate clockwise.

We illustrate the leaves of f_1 and arrow decorations near the $2(b-1)$ resulting \times -singularities in the left half of Figure 13.

In the right half of Figure 13 we draw an alternative view of the leaves of f_1 ; the first view will be more useful but it might be easier for a reader to see that the second arises from applying $b-1$ instances of the movie of Example 4.1 to f_0 . The two images of Figure 13 are related by an isotopy that rotates horizontal pairs of boundary components through 180° , exchanging the two boundaries.

5.2. Step 2: fibering $h|_M^{-1}[1, 2]$. Let $1 = t_1 < t_2 < \dots < t_n < t_{n+1} = 2$ so that β meets $h^{-1}[t_i, t_{i+1}]$ in a braid described by the i -th letter w_i of w . Our goal is to extend f_t across each $[t_i, t_{i+1}]$ by viewing the i -th crossing of β as a band move and applying the band movie of Example 4.3.

Say $w_1 = \sigma_j^{s_j}$. In the left of Figure 14, we illustrate an open set of $h|_M^{-1}(1)$ that has boundary circles $C_{j-1}, C_{j-1}', C_j, C_j', C_{j+1},$ and C_{j+1}' . (If $j = 1$, then ignore the top portion including C_{j-1}, C_{j-1}' .) We assume $s_j = 1$; the $s_j = -1$ case is similar (mirror along a horizontal axis and take the included boundary components to be $C_j, C_j', C_{j+1}, C_{j+1}', C_{j+2}, C_{j+2}'$). This subspace is easily visible in the left of Figure 13. We give two cases, depending on the sign of s_{j-1} . In Figure 14, we illustrate how to extend f_t across $t \in [1, t_2]$. We first perform a band movie along the illustrated arc η . (One can check that the endpoints of η can be taken to have the same image under f_1 , as required.) Then C_j, C_{j+1} exchange positions as t increases, after which we exchange their labels. We see that the contour set of f_{t_2} agrees with f_1 away from a disk containing $C_j, C_j', C_{j+1}, C_{j+1}'$.

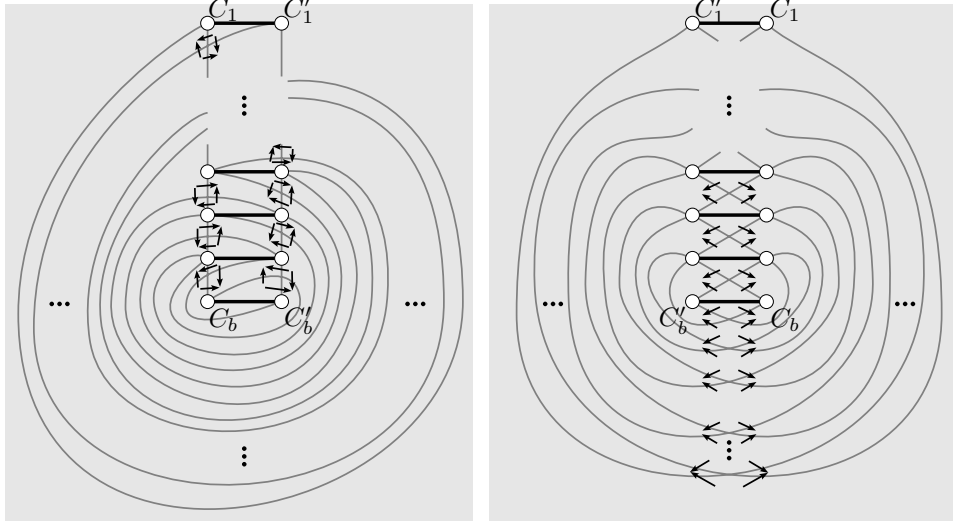


FIGURE 13. **Left:** A contour map of f_1 as obtained in Step 1. From top to bottom, the horizontal pairs of boundary components are near A_1, \dots, A_b . In this figure, we have assumed $s_1 = 1, s_{b-4} = 1, s_{b-3} = -1, s_{b-2} = -1, s_{b-1} = 1$. The left column of boundary components from top to bottom are C_1, \dots, C_b , while the right column of boundary components are from top to bottom C'_1, \dots, C'_b . In bold, we draw the projections of the arcs $L \cap B_-^3$ to $h|_M^{-1}(1)$. Each of these arcs is in a level set of f_1 . **Right:** Another contour map obtained by isotoping the lefthand diagram. This isotopy rotates each pair C_i, C'_i ($i = 2, \dots, b$) through 180° in the direction determined by s_i , exchanging the two boundary components.

We similarly extend f_t along each interval $t \in [t_i, t_{i+1}]$ unless the letter w_i has already appeared in w . In this case, suppose $w_i = \sigma_j^{s_j}$ and $w_k = \sigma_j^{s_j}$ for some $k < i$. Then we must have performed the above operation in a neighborhood of $C_j, C'_j, C_{j+1}, C'_{j+1}$ when extending f_t along $t \in [t_k, t_{k+1}]$. Therefore, the leaves of f_{t_i} have the local model of Figure 14 (right), again assuming $s_j = 1$ (the case $s_j = -1$ is similar). In Figure 15, we show how to extend f_t to $t \in [t_i, t_{i+1}]$. We perform the indicated band move and obtain a singular fibration that agrees with the middle stage of Figure 14, and then proceed as in Figure 14.

Thus, we may inductively extend f_t over $t \in [t_i, t_{i+1}]$ for increasing i . If w_i is the first instance of $\sigma_j^{s_j}$ in w , then we use the movie of Figure 14 (mirrored along a horizontal axis if $s_j = -1$). If w_i is not the first instance of $\sigma_j^{s_j}$, then we use the movie illustrated in Figure 15 (again mirrored if $s_j = -1$).

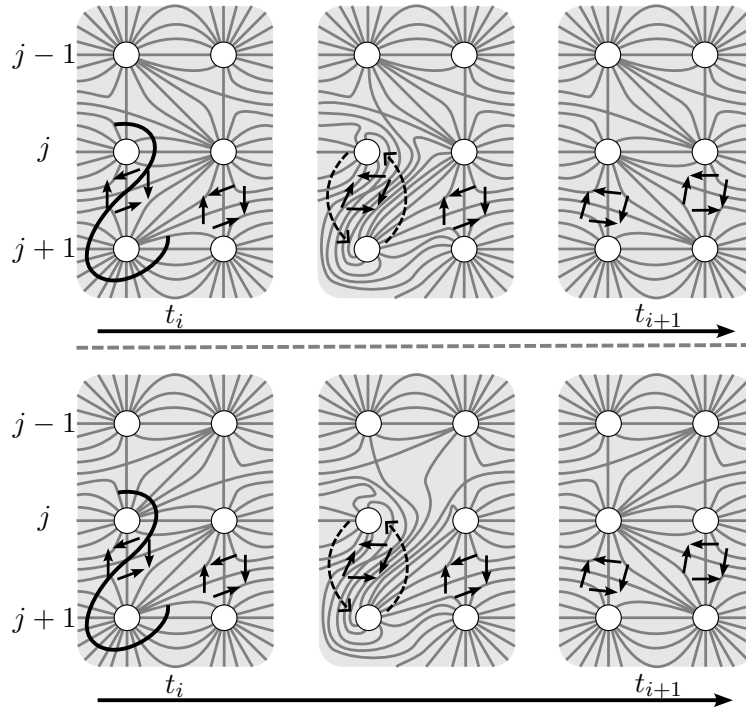


FIGURE 14. Here we assume $s_j = 1$. We give two possible local models depending on the behavior of f_{t_i} in a box containing $C_{j-1}, C'_{j-1}, C_j, C'_j$. This depends on the sign of s_{j-1} and whether we have already extended f_t across some interval corresponding to $\sigma_{j-1}^{s_{j-1}}$. **Left:** An open subset of $h_M^{-1}(t_i)$. We include an arc η satisfying the conditions of the band movie. **Middle:** We perform a band movie and indicate with dashed arrows the path of C_j, C_{j+1} as we move above the crossing of β corresponding to w_i . **Right:** An open subset of $h_M^{-1}(t_{i+1})$.

Because every $\sigma_j^{s_j}$ appears at least once in w , the singular fibration f_2 is as in Figure 16.

5.3. Step 3: fibering $B_+^3 \setminus \nu(L)$. We have so far extended f_t to a movie of singular fibrations on M for $t \leq 2$.

While f_1 and f_2 (Figures 13 and 16) seem similar, there is a key difference between these two singular fibrations. Projections of the arcs $L \cap B_-^3$ to $h_M^{-1}(1)$ form a level set of f_1 that lies toward *outward* regions of the \times -singularities, as in the movie of Example 4.1. However, projections of arcs in $L \cap B_+^3$ to $h_M^{-1}(2)$ form a level set of f_2 that lies toward *inward* regions of the \times -singularities, as in the movie of Example 4.2. We may thus extend f_t across $t \in [2, 3]$ by applying $b - 1$ instances of the movie of Example 4.2. (Note this is exactly the same as our procedure to extend f_t along $t \in [0, 1]$)

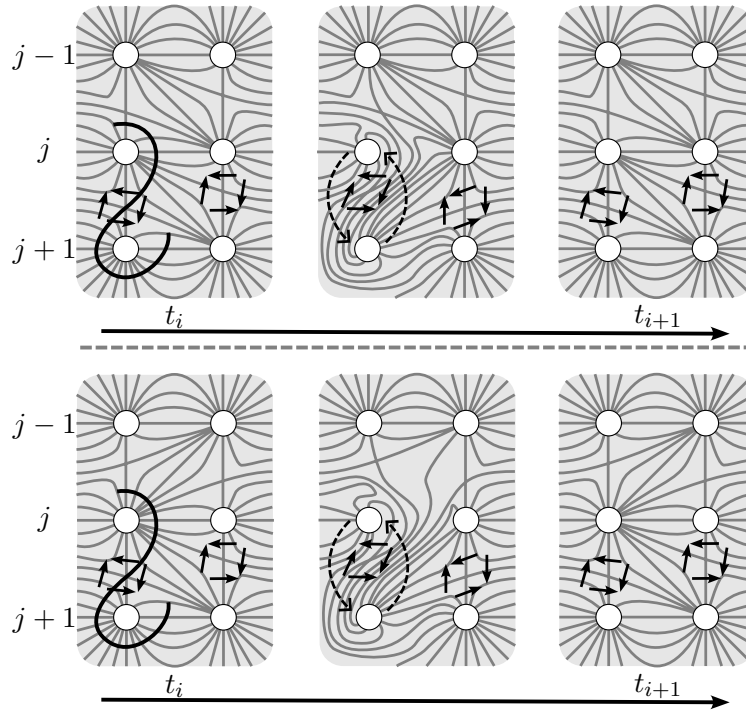


FIGURE 15. Here, $s_j = 1$ and $w_i = \sigma_j^{s_j}$ is not the first instance of $\sigma_j^{s_j}$ in w . We give two cases (top row and bottom row), depending on the behavior of f_{t_i} in a disk containing $C_{j-1}, C'_{j-1}, C_j, C'_j$. (That is, depending on the sign of s_{j-1} and whether $\sigma^{s_{j-1}}$ appears in the first $i-1$ letters of w .) **Left:** a local model of f_{t_i} . We indicate an arc along which we may perform a band move. **Middle:** We perform the band move. Note that this singular fibration agrees with that of the middle of 14. **Right:** An open subset of $h_M^{-1}(t_{i+1})$.

from Step 1, turned upside down, so we abbreviate the discussion.) Then f_3 is a fibration of an annulus over S^1 . We extend f_t across $t \in [3, \infty)$ via the movie of Figure 11 used in Step 1, turned upside down with respect to t . This concludes the construction of f_t and hence the proof of Theorem 1.2.

6. EXAMPLE OF A FIBRATION

In Figures 17 and 18, we perform the above algorithm to construct a fibration $F : S^3 \setminus (\text{right-handed trefoil}) \rightarrow S^1$. In Figure 17 we draw the contour set of each $f_t := F|_{h^{-1}(t)}$. In Figure 18 we highlight $F^{-1}(\theta)$ for three values of θ . Each of these leaves can be easily seen to be the standard braid surface (as expected). Note that, as stated in Theorem 1.2, h restricts to the interior of each $F^{-1}(\theta)$ as a Morse function with no local minima or maxima.

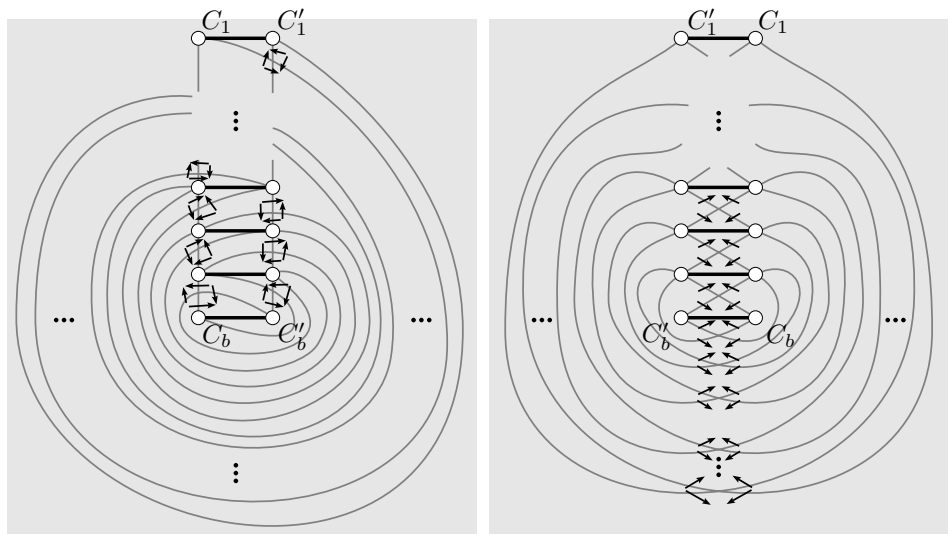


FIGURE 16. **Left:** A contour map of f_2 as obtained in Step 2. From top to bottom, the horizontal pairs of boundary components are $C_1, C'_1; \dots, C_b, C'_b$. As in Figure 13, in this figure we have assumed $s_1 = 1, s_{b-4} = 1, s_{b-3} = -1, s_{b-2} = -1, s_{b-1} = 1$. In bold, we draw the projections of the arcs $L \cap B_+^3$ to $h|_M^{-1}(2)$. **Right:** Another contour map obtained by isotoping the lefthand diagram, included only for visualization purposes. This isotopy rotates each pair C_i, C'_i ($i = 2, \dots, b$) through 180° in the direction determined by s_i , exchanging the two boundary components.

REFERENCES

- Mil21. Maggie Miller. Extending fibrations of knot complements to ribbon disk complements. *Geom. Topol.*, 25(3):1479–1550, 2021.
- Ni07. Yi Ni. Knot Floer homology detects fibred knots. *Invent. Math.*, 170(3):577–608, 2007.
- Sta78. John R. Stallings. Constructions of fibred knots and links. In *Algebraic and geometric topology (Proc. Sympos. Pure Math., Stanford Univ., Stanford, Calif., 1976), Part 2*, Proc. Sympos. Pure Math., XXXII, pages 55–60. Amer. Math. Soc., Providence, R.I., 1978.

DEPARTMENT OF MATHEMATICS, STANFORD UNIVERSITY, STANFORD, CA 94301, USA

Email address: maggie.miller.math@gmail.com

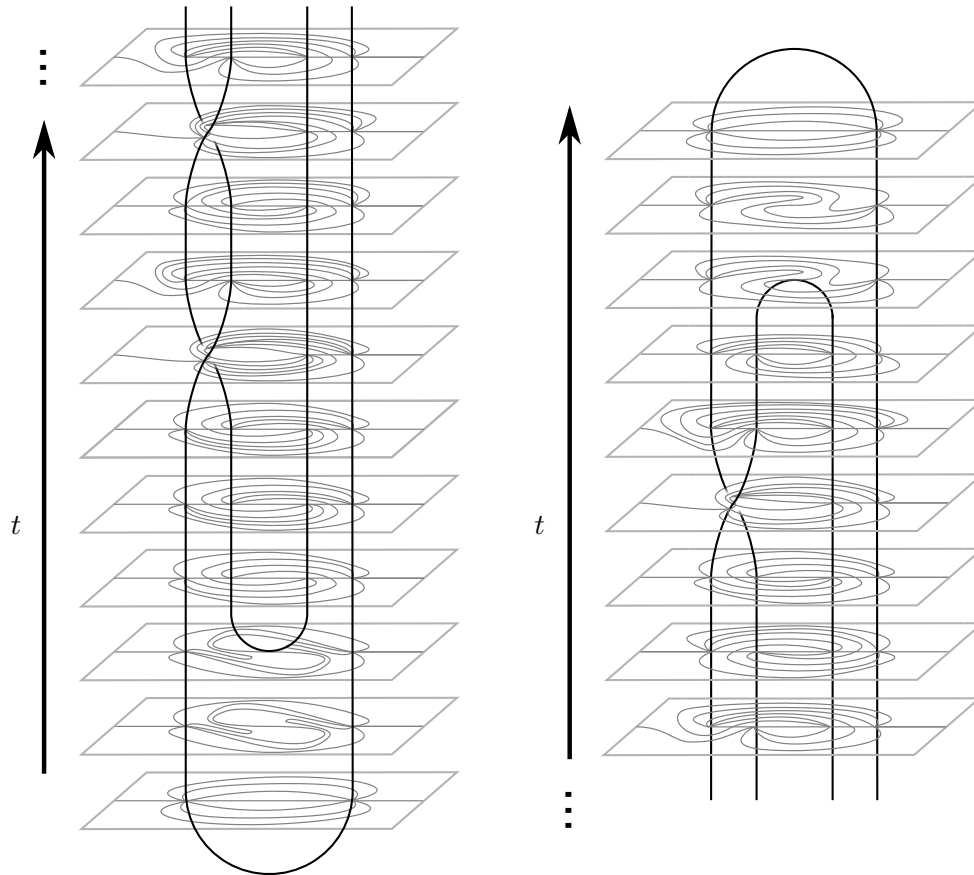


FIGURE 17. A contour set for f_t for increasing t , where f_t is a movie of singular fibrations on the trefoil complement with total function F a fibration. This movie has been constructed via the algorithm of Theorem 1.2.

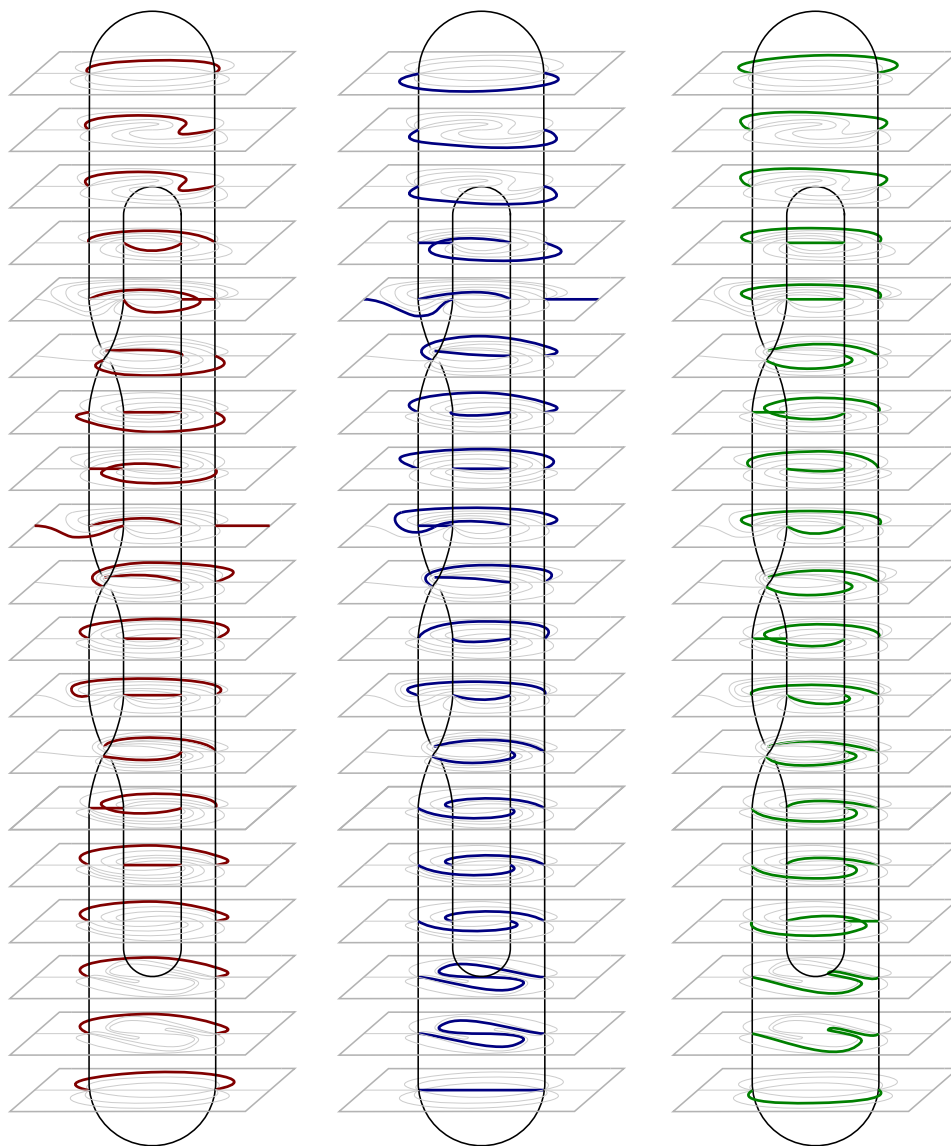


FIGURE 18. Three fibers $F^{-1}(\theta)$ for the trefoil, constructed as in Theorem 1.2.